Reactions of Methane with Hafnium Atoms: CH_2=HfH_2, Agostic Bonding, and $(CH_3)_2HfH_2$

Han-Gook Cho, Xuefeng Wang, and Lester Andrews*

Department of Chemistry, University of Virginia, P.O. Box 400319, Charlottesville, Virginia 22904-4310

Received January 31, 2005

Laser-ablated hafnium atoms react with methane to form the methylidene complex CH_2=HfH_2. The activation of a second CH_4 molecule forms $(CH_3)_2HfH_2$ particularly on sample annealing. These molecules are identified from infrared spectra by isotopic substitution (CH_4, $^{13}CH_4$, CD_4, CH_2D_2) and comparison to DFT frequency calculations. The computed structure for singlet ground state CH_2=HfH_2 shows CH_2 and HfH_2 distortion and evidence for agostic bonding (angle H−C−Hf, 95.6°), which is more stable than the symmetrical nonagostic structure. The CHD=HfHD isotopic molecules provide experimental evidence for agostic bonding distortion. In addition, changes within the absorptions of the CHD=HfHD isotopic molecules on annealing the argon matrix to 20−26 K demonstrates facile interchange of the agostic bonding positions.

Introduction

Alkylidene complexes containing carbon−metal double bonds are of interest as catalysts for methane activation and for understanding the fundamental metal−carbon interaction.[1,2] The selective activation of C−H of alkanes using transition metal catalyst systems is an important step in the production of useful products.

Agostic bonding has been discovered in a number of early transition metal alkylidene complexes, and these simple systems provide a basis to characterize the agostic interaction.[2] The simplest such molecule is the methylene dihydride complex, CH_2=MH_2, which is a very good model system to investigate substituent effects on the agostic interaction.[3−6] Several substituted methylidenes of this type have been explored by early electronic structure calculations using minimum basis sets, which found symmetrical CH_2 structures and no evidence for agostic distortion.[7,8] Recently, we have reacted Ti and Zr atoms with CH_4 and prepared CH_2=TiH_2 and CH_2=ZrH_2 for spectroscopic examination: The observed frequencies match frequencies calculated for distorted, agostic molecules, and the CHD=MHD isotopic molecules show inequivalent H(D) atoms on the metal centers.[9−11] It is necessary to include polarization functions on carbon in the basis set in order to describe the agostic interaction.[4,9,10] These simple methylidene complexes containing carbon−metal double bonds are special examples of more complicated ligated complexes.[12,13]

Methyl halides are more reactive with electron-deficient group 4 transition metal atoms than CH_4, and several CH_2=MHX methylidene complexes have been prepared and their structures computed.[10,11] We find that the agostic interaction increases in the series CH_2=TiHX (X = F, Cl, Br) but decreases in the series CH_2=MHF (M = Ti, Zr, Hf).[14−16,18] These systems also activate a second CH_4 or CH_3X molecule to form $(CH_3)_2TiH_2$, $(CH_3)_2ZrH_2$, $(CH_3)_2TiF_2$, $(CH_3)_2TiCl_2$, and $(CH_3)_2TiBr_2$.[10,11,17,18] The related $(Cp^*)_2HfH_2$ compound has been prepared and investigated.[19] Therefore, we expect the $(CH_3)_2HfH_2$ molecule to be a stable reaction product.

Experimental and Computational Methods

The laser-ablation matrix-infrared experiment has been described previously.[20,21] Briefly, laser-ablated hafnium atoms (Johnson-Matthey) were reacted with CH_4 (Matheson, UHP grade), $^{13}CH_4$, CD_4, and CH_2D_2 (Cambridge Isotopic Laboratories) in excess neon (Spectra Gases) or argon (MG Industries) during condensation on a CsI window at 5 or 8 K. Infrared

* To whom correspondence should be addressed. E-mail: lsa@virginia.edu.

(1) Buchmeiser, M. R. *Chem. Rev*. **2000**, *100*, 1565.
(2) Schrock, R. R. *Chem. Rev*. **2002**, *102*, 145.
(3) Crabtree, R. H. *Chem. Rev.* **1985**, *85*, 245.
(4) Ujaque, G.; Cooper, A. C.; Maseras, F.; Eisenstein, O.; Caulton, K. G. *J. Am. Chem. Soc*. **1998**, *120*, 361.
(5) Wada, K.; Craig, B.; Pamplin, C. B.; Legzdins, P.; Patrick, B. O.; Tsyba, I.; Bau, R. *J. Am. Chem. Soc*. **2003**, *125*, 7035.
(6) Bau, R.; Mason, S. A.; Patrick, B. O.; Adams, C. S.; Sharp, W. B.; Legzdins, P. *Organometallics* **2001**, *20*, 4492.
(7) (a) Franci, M. M.; Pietro, W. J.; Hout, R. F., Jr.; Hehre, W. J. *Organometallics* **1983**, *2*, 281. (b) Franci, M. M.; Pietro, W. J.; Hout, R. F., Jr.; Hehre, W. J. *Organometallics* **1983**, *2*, 815.
(8) Cundari, T. R.; Gordon, M. S. *J. Am. Chem. Soc*. **1992**, *114*, 539.
(9) Andrews, L.; Cho, H.-G.; Wang, X. *Angew. Chem.* **2005**, *117*, 115.
(10) Cho, H.-G.; Wang, X.; Andrews, L. *J. Am. Chem. Soc.* **2005**, *127*, 465.
(11) Andrews, L.; Cho, H.-G.; Wang, X. *Inorg. Chem.* **2005**, in press. (Ti+CH_4).
(12) Fryzuk, M. D.; Mao, S. S. H.; Zaworotko, M. J.; McGillivray, L. R. *J. Am. Chem. Soc.* **1993**, *115*, 5336.
(13) Fryzuk, M. D.; Duval, P. B.; Patrick, B. O.; Rettig, S. J. *Organometallics* **2001**, *20*, 1608.
(14) Cho, H.-G.; Andrews, L. *J. Phys. Chem. A* **2004**, *108*, 6294.
(15) Cho, H.-G.; Andrews, L. *J. Am. Chem. Soc.* **2004**, *126*, 10485.
(16) Cho, H.-G.; Andrews, L. *Organometallics* **2004**, *23*, 4357.
(17) Cho, H.-G.; Andrews, L. *Inorg. Chem.* **2005**, *44*, 979.
(18) Cho, H.-G.; Andrews, L. *Inorg. Chem.* **2004**, *43*, 5253.
(19) Roddick, D. M.; Fryzuk, M. D.; Seidler, P. F.; Hillhouse, G. L.; Bercaw, J. E. *Organometallics* **1985**, *4*, 97.
(20) Chertihin, G. V.; Andrews, L. *J. Phys. Chem*. **1995**, *99*, 6356 (HfO_2).
(21) Andrews, L.; Citra, A. *Chem. Rev.* **2002**, *102*, 885, and references therein.

10.1021/om050069l CCC: $30.25
Publication on Web 05/04/2005

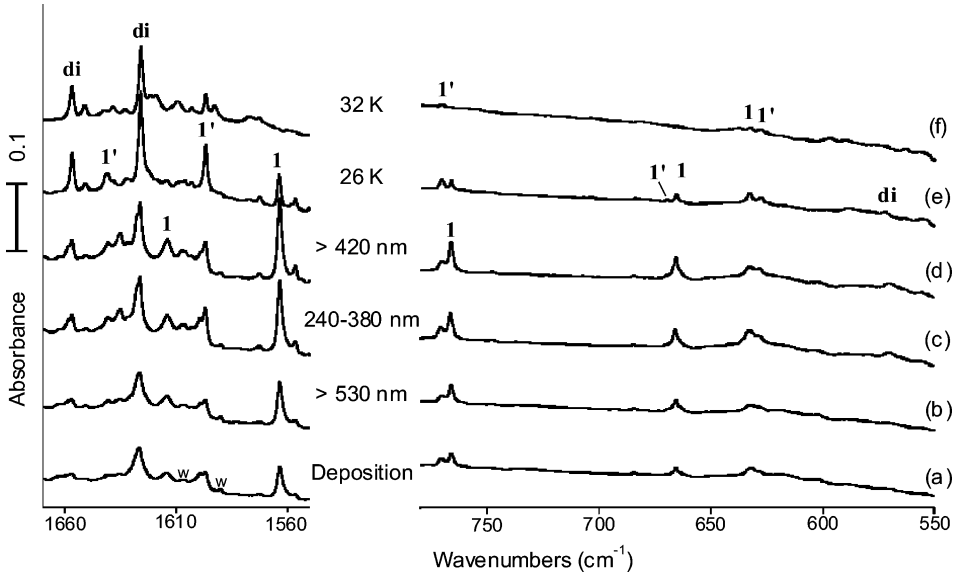

Figure 1. Infrared spectra in the 1670−1550 and 780−550 cm^{-1} regions for laser-ablated Hf reaction products with 2% CH_4 in argon at 7 K: (a) sample co-deposition for 60 min, (b) after $\lambda > 530$ nm irradiation for 20 min, (c) after 240−380 nm irradiation, (d) after $\lambda > 420$ nm irradiation, (e) after annealing to 26 K, and (f) after annealing to 32 K. W denotes water impurity.

spectra were recorded at 0.5 cm^{-1} resolution on Nicolet Magna spectrometers with HgCdTe detectors. Samples were irradiated by a mercury arc lamp (175 W, globe removed) for 20 min periods and annealed, and more spectra were recorded.

Density functional theory (DFT) calculations for expected reaction products were done using the Gaussian 98 package,[22] B3LYP density functional, and medium 6-311++G(2d,p) and large 6-311++G(3df,3pd) basis sets for C and H, and the SDD Stuttgart/Dresden effective core potential and basis set for Hf (12 valence electrons),[23] to provide a consistent set of vibrational frequencies for the reaction products. Geometries were fully relaxed during optimization, and the optimized geometry was confirmed to be a true minimum by vibrational analysis with no imaginary frequencies. All vibrational frequencies were calculated analytically. Calculations were also done with the MP2 method for comparison.

Results

Experiments with Hf and CH_4 in excess argon and neon and DFT calculations of expected reaction products will be presented.

Argon Matrix. Experiments were performed with laser-ablated Hf and CH_4 in excess argon at 0.5 and 2% concentrations, and infrared spectra from the latter investigation are illustrated in Figure 1. New absorptions are observed at 1657.3, 1626.6, and 570.0 cm^{-1} (labeled **di**) plus 1377.8 and 1142.2 cm^{-1} (not shown) and band pairs at 1641.2, 1614.2, 1597.1, 1563.6, 770.7, 766.3, 669.7, 665.8, 632.6 and 627.9 cm^{-1} (labeled **1′** and **1**). Successive visible, UV, and visible irradiations (Figure 1b,c,d) consistently increased the **1** bands and the **di** absorptions and slightly increased, and decreased, the **1′** bands. Next, annealing to 20 and to 26 K favored the **1′** bands over the **1** bands and markedly increased the **di** bands, much like that found in the zirconium/methane system.[9,10] Similar behavior was obtained with 0.5% CH_4, but the **di** bands were half as intense relative to the **1** bands. In addition, weak HfO_2 absorptions[20] were observed, which attests that the reacting metal species is atomic hafnium.

Isotopic substitution of the methane precursor provided important spectroscopic information, which is listed in Table 1. Spectra from the $^{13}CH_4$ and CD_4 experiments are shown in Figures 2 and 3. Carbon-13 substitution had no significant effect on the bands in the upper region, but small shifts were observed in the lower region. All bands shifted with CD_4 by larger factors in the upper than in the lower region.

The CH_2D_2 reagent gave additional new diagnostic absorptions in the Hf−H and Hf−D stretching regions as shown in Figure 4. The initial bands observed at 1563.4 and 1120.9 cm^{-1} (labeled **2** and **7**) are virtually unshifted from CH_4 and CD_4 values. Next visible and UV irradiations increase these bands and bring along new counterparts at 1579.6 and 1130.7 cm^{-1} (marked **4**, **6**), and the bands at 1596.5 and 1144.5 cm^{-1} have two new counterparts each at 1615.4, 1606.1 cm^{-1} and at 1157.4, 1151.1 cm^{-1} (marked **4′**, **6′** and **3′**, **5′**). Annealing to 20 and to 26 K decreases the **2** and **7** bands and increases the **4′**, **6′** and **3′**, **5′** bands, and markedly increases the **di** bands now at 1657.1 and 1626.1 cm^{-1} with a stronger intermediate component at 1641.1 cm^{-1} and at 1184.7 and 1165.5 cm^{-1} with a stronger middle component at 1175.3 cm^{-1}. Final annealing to 32 K decreased the **2** and **7** bands much more than the **di** absorptions.

(22) Frisch, M. J.; Trucks, G. W.; Schlegel, H. B.; Scuseria, G. E.; Robb, M. A.; Cheeseman, J. R.; Zakrzewski, V. G.; Montgomery, J. A., Jr.; Stratmann, R. E.; Burant, J. C.; Dapprich, S.; Millam, J. M.; Daniels, A. D.; Kudin, K. N.; Strain, M. C.; Farkas, O.; Tomasi, J.; Barone, V.; Cossi, M.; Cammi, R.; Mennucci, B.; Pomelli C.; Adamo, C.; Clifford, S.; Ochterski, J.; Petersson, G. A.; Ayala, P. Y.; Cui, Q.; Morokuma, K.; Rega, N.; Salvador, P.; Dannenberg, J. J.; Malick, D. K.; Rabuck, A. D.; Raghavachari, K.; Foresman, J. B.; Cioslowski, J.; Ortiz, J. V.; Baboul, A. G.; Stefanov, B. B.; Liu, G.; Liashenko, A.; Piskorz, P.; Komaromi, I.; Gomperts, R.; Martin, R. L.; Fox, D. J.; Keith, T.; Al-Laham, M. A.; Peng, C. Y.; Nanayakkara, A.; Challacombe, M.; Gill, P. M. W.; Johnson, B.; Chen, W.; Wong, M. W.; Andres, J. L.; Gonzalez, C.; Head-Gordon, M.; Replogle, E. S.; Pople, J. A. *Gaussian 98*, Revision A.11.4; Gaussian, Inc.: Pittsburgh, PA, 2002.

(23) (a) Krishnan, R.; Binkley, J. S.; Seeger, R.; Pople, J. A. *J. Chem. Phys*. **1980**, *72*, 650. (b) Frisch, M. J.; Pople, J. A.; Binkley, J. S. *J. Chem. Phys.* **1984**, *80*, 3265. (c) Andrae, D.; Haeussermann, U.; Dolg, M.; Stoll, H.; Preuss, H. *Theor. Chim. Acta* **1990**, *77*, 123.

Table 1. Frequencies Observed for Hf + CH_4 Product Absorptions[a]

group	CH_4		CD_4		$^{13}CH_4$	CH_2D_2			description
1′	1641.2	(1653.5)	1165.7		1641.2	1615.4,	1606.1		sym. HfH_2 str.
1	**1614.2**		**1153.3**		1614.1	1157.4,	1151.1		
1′	1597.1	(1632.3)	1144.4	(1169.6)	1597.0	1596.5	**1579.6**	1144.5	
1	**1563.6**	(1616.3)	1120.9	(1158.5)	1563.5	**1563.4**	**1120.9**	**1130.7**	antisym. HfH_2 str.
	770.7, **766.3**	(773.4)	673.0, 674.9		**748.0**, 750.6	**718.4**	**754.4**	**723.4**	C=Hf str.
	669.7, **665.8**		**534.5**, 527.9		**660.6**	**531.1**	**666.7**	**547.9, 555.9**	CH_2 wag
	632.6, 627.9				**629.6**, 624.7	729.6	765.2	527.9, **645**	HfH_2 bend
di	1657.3	(1670.2)	1184.5	(1194.3)	1657.2	1657.1	1641.1	1626.1	HfH_2 str. (A)
	1626.6	(1640.9)	1163.4	(1176.4)	1626.5	1184.7	1175.3	1165.5	HfH_2 str. (B)
	1377.8	(1380.5	CD_4[b]	(CD_4)[b]	1374.3	1615.4,	1606.1		CH_3 scis. (B)
	1142.2	(1145.2)		(902.0)	1131.6	1157.4,	1151.1		CH_3 deform (B)
	570.0	(576.5)		(467.6)	566.8				HfH_2 wag (B)

[a] All frequencies are in cm^{-1}. The first argon matrix absorptions are bolded. Parentheses denote neon matrix frequencies. [b] CD_4 masks any product absorption near 1000 cm^{-1}.

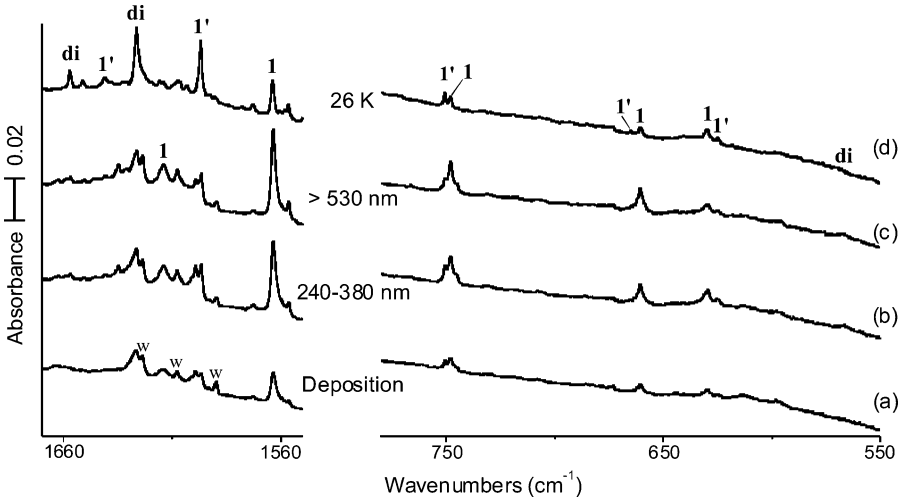

Figure 2. Infrared spectra in the 1670−1550 and 780−550 cm^{-1} regions for laser-ablated Hf reaction products with 0.5% $^{13}CH_4$ in argon at 7 K: (a) sample co-deposition for 60 min, (b) after 240−380 nm irradiation, (c) after $\lambda > 530$ nm irradiation for 20 min, and (d) after annealing to 26 K. W denotes water impurity.

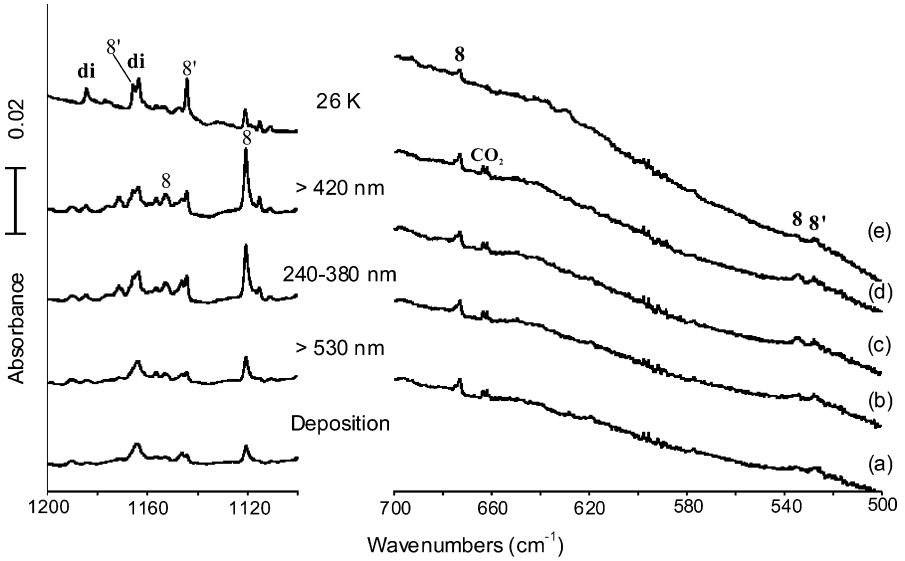

Figure 3. Infrared spectra in the 1200−1100 and 700−500 cm^{-1} regions for laser-ablated Hf reaction products with 0.5% CD_4 in argon at 7 K: (a) sample co-deposition for 60 min, (b) after $\lambda > 530$ nm irradiation for 20 min, (c) after 240−380 nm irradiation, (d) after $\lambda > 420$ nm irradiation, and (e) after annealing to 26 K.

Neon Matrix. Hf reactions were done with CH_4 and CD_4 in excess neon, and a representative spectrum is illustrated in Figure 5. The initial co-deposit for 0.4% CH_4 revealed a sharp, weak **1** band at 1616.3 beside the 1614.2 cm^{-1} water absorption, and weak, broad **di** bands at 1673 and 1643 cm^{-1}. These bands increased on visible irradiation, and the latter markedly increased on UV irradiation (Figure 5c). Annealing to 10.5 K sharpened the latter to 1670.2 and 1640.9 cm^{-1}, and annealing to 11.5 K decreased the **1** band in favor of a

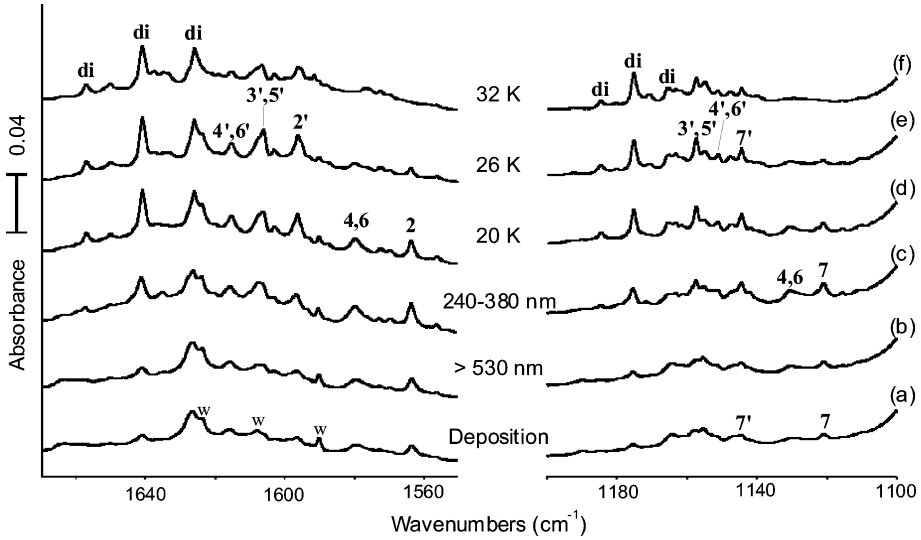

Figure 4. Infrared spectra in the 1670−1550 and 1200−1100 cm^{-1} regions for laser-ablated Hf reaction products with 2% CH_2D_2 in argon at 7 K: (a) sample co-deposition for 60 min, (b) after $\lambda > 530$ nm irradiation for 20 min, (c) after 240−380 nm irradiation, (d) after annealing to 20 K, (e) after annealing to 26 K, and (f) after annealing to 32 K. W denotes water impurity.

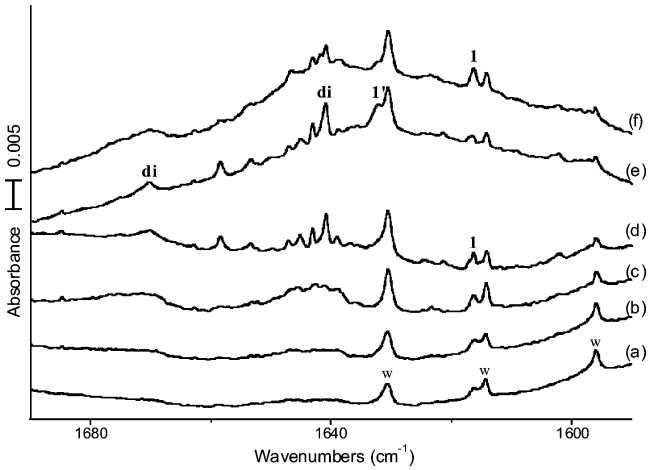

Figure 5. Infrared spectra in the Hf−H stretching region for products of laser-ablated Hf atom reactions with 0.4% CH_4 in neon: (a) sample deposited for 60 min, (b) after $\lambda > 530$ nm irradiation for 20 min, (c) after 240−380 nm irradiation, (d) after annealing to 10.5 K, (e) after annealing to 11.5 K, and (f) after $\lambda > 220$ nm irradiation. W denotes water impurity.

1′ counterpart at 1632.3 cm^{-1} (Figure 5e). A final full arc irradiation reduced the **di** bands and the **1′** band in favor of the original **1** absorption. Additional **di** bands and CD_4 counterpart absorptions are listed in Table 1.

Calculations. DFT calculations were done at the B3LYP/6-311++G(2d,p)/SDD level for anticipated reaction products, and the structures are illustrated in Figure 6. Additional geometrical parameters are given in Table S1. The singlet ground state methylidene dihydride $CH_2{=}HfH_2$ is almost planar at carbon, but clearly pyramidal at Hf, has inequivalent H atoms at the C and Hf centers (agostic H−C−Hf angle 98.4°), and is 21.2 kcal/mol more stable than $Hf(^3F)+CH_4$. Calculation with the MP2 method (Table S1) gives a shorter C=Hf bond and a still smaller (81.6°) agostic angle and reasonable frequencies. The $^3A''$ state CH_3HfH insertion product and $(CH_3)_2HfH_2$ molecule have almost the same C−Hf bond lengths, but the higher metal oxidation state compound has shorter computed Hf−H bonds and higher frequency vibrational modes. The triplet CH_3HfH molecule is 21.8 kcal/mol more stable than Hf + CH_4, and $(CH_3)_2HfH_2$ is bound by 72.3 kcal/mol. We find $CH_2{=}HfH_2$ to be more strongly bound by 10.6 kcal/mol than CH_3-HfH at the MP2 level.

Frequencies computed for CH_3HfH are listed in Table 2. The Hf−H stretch at 1634 cm^{-1} is a strong mode, and the weaker C−Hf−H bending mode at 544 cm^{-1} might be observable. Frequencies calculated for $CH_2{=}HfH_2$ isotopic molecules are listed in Table 3: Five modes have sufficient intensity to be observed in these experiments. Frequencies were also computed for the four CHD=HfHD isotopic variants shown in Chart 1 for later comparisons. Calculated and observed values for five intense frequencies in the infrared spectrum of $(CH_3)_2HfH_2$ are listed in Table 4. Another interesting possibility, CH_3-HfH_3, was also computed, and this C_{3v} singlet ground state has two strong Hf−H stretching modes (1726 cm^{-1}, 163 km/mol; 1681 cm^{-1}, 526 × 2 km/mol).

The argon complex with $CH_2{=}HfH_2$ is computed to be bound by 2.6 kcal/mol at the MP2 level of theory (large basis for C and H, and SDD for Hf and Ar), which is due in part to the large charge on Hf (Table S1) and the availability of the Hf center for complex formation. The argon complex results in only slight distortion of $CH_2{=}HfH_2$ and +5 to −9 cm^{-1} shifts in the most intense IR absorbing modes. The argon complex with two Ar bound to Hf above and below the $CH_2{=}HfH_2$ plane is more stable by 0.7 kcal/mol, and again the molecule is changed very little (agostic angle still 81.6°) and the Hf−H stretching modes continue to red shift while the other strong modes blue shift.

The group 4 methylidene dihydride structures were recomputed with the large 6-311++G(3df,3pd) basis for C and H and the SDD pseudopentential and basis for the metals. These structures are compared in Figure 7: Notice that calculation with additional polarization functions gives a slightly shorter C=Hf bond, smaller H−C−Hf angle, and increased difference between C−H and Hf−H bond lengths, i.e., more agostic distortion.

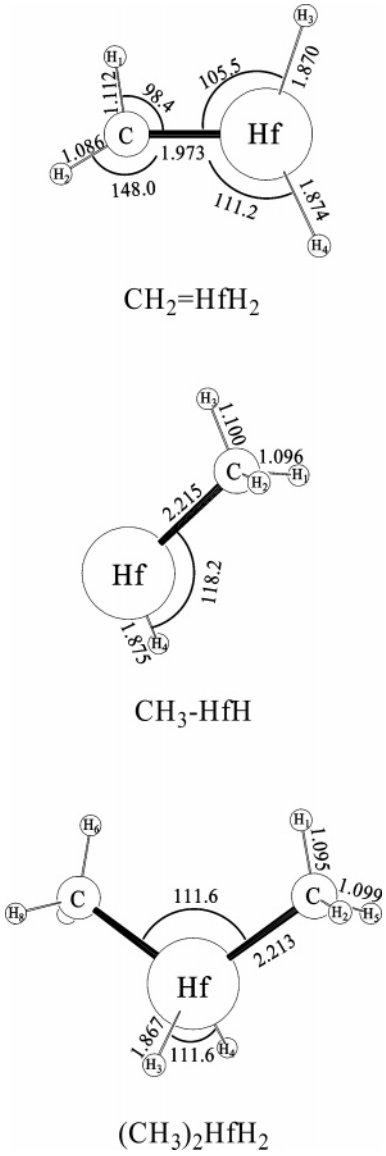

Figure 6. Structures computed for hafnium methylidene complexes and hydrides at the B3LYP/6-311++G(2d,p)/SDD level.

Table 2. Calculated Frequencies (cm^{-1}) for CH_3HfH in the Triplet Ground State[a]

approximate mode	$^{12}CH_3-HfH$	$^{13}CH_3-HfH$
C−H stretch	3053.6 (a′, 6)[b]	3043.2
C−H stretch	3019.1 (a″, 6)	3008.7
C−H stretch	2956.3 (a′, 7)	2953.1
Hf−H stretch	1633.5 (a′, 365)	1633.5
C−H_2 bend	1417.4 (a′, 4)	1414.3
C−H_2 bend	1417.1 (a″, 7)	1414.0
C−H bend	1163.2 (a′, 22)	1153.3
C−Hf−H bend	544.2 (a′, 47)	538.5
C−Hf stretch	477.5 (a′, 12)	437.3
CH_3 motion	385.1 (a″, 3)	383.2
CH_3 motion	291.4 (a′, 14)	291.2
CH_3 motion	186.5 (a″, 11)	186.5

[a] Calculated at the B3LYP/6-311++G(2d,p)/SDD level. [b] a′ or a″ mode in C_s symmetry; infrared intensity, km/mol.

Also notice that the H−C−M angle increases from Ti to Zr to Hf. Natural bond orbital analysis[24] was done for this methylidene complex family, and the computed charges and natural electron configurations are summarized in Table 5.

Discussion

The molecular products of methane activation by Hf will be identified from matrix infrared spectra and DFT calculations.

CH_2=HfH_2. The first product anticipated is the metal-inserted CH_3HfH hydride, which has essentially the same energy as the methylidene complex at the B3LYP level but is 10.6 kcal/mol higher in energy at the MP2 level (Table S1). We observe no product absorptions that are appropriate for the inserted species[10,11,14,15,17] in the 1550−1400 and 550−500 cm^{-1} regions where CH_3HfH should appear based on calculated frequencies and comparison with CH_2=HfH_2. The product absorption subgroups labeled **1** and **1′** each contain symmetric and antisymmetric Hf−H stretching, C=Hf stretching, CH_2 wagging, and H−Hf−H bending modes, which require the methylidene structure, as comparison of calculated and observed **1** subgroup absorptions in Table 3 shows. First, the 1614.2 and 1563.6 cm^{-1} bands are Hf−H(D) stretching modes, as their H/D ratios (1.400, 1.395) and lack of ^{13}C shift demonstrate.[25] However, the 766.3 cm^{-1} band shifts to 748.0 cm^{-1} with $^{13}CH_4$ (Figure 2), and this mostly C=Hf stretching mode computed at 751.7 cm^{-1} is predicted to shift 17.8 cm^{-1} with ^{13}C. This mode is mixed with H−Hf−H bending, as it also shows a substantial deuterium shift to 684.4 cm^{-1}. Next the associated 665.8 cm^{-1} band has a small (observed 5.2 cm^{-1}, calculated 7.7 cm^{-1}) ^{13}C shift and a large (observed 131.3 cm^{-1}, harmonic calculated 144.5 cm^{-1}) deuterium shift (Figure 3), which are appropriate for the CH_2 wagging motion. The 632.6 cm^{-1} band also shows a small ^{13}C shift (observed 3.0 cm^{-1}, calculated 3.2 cm^{-1}) for this mostly H−Hf−H bending mode. Similar comparisons can be made with the related **1′** subgroup absorptions at 1640.9, 1597.1, 770.7, and 669.7 cm^{-1}. In conclusion, the agreement between calculated and observed CH_2=HfH_2 frequencies (Table 3) supports our preparation and identification of the methylidene hafnium dihydride complex (1 in Chart 1). Similar observations and computations[10] for CH_2=ZrH_2 also support this finding.

The CH_2D_2 reaction products provide confirming evidence. Chart 1 illustrates the six possible methylidene products that can be made from CH_2D_2, and the computed frequencies in Table 3 show that CD_2=HfH_2 and CH_2=HfD_2 have common antisymmetric metal−hydride stretching frequencies with the pure isotopic species. However, the strongest frequencies computed for the four CHD=HfHD modifications (3, 4, 5, and 6 in Chart 1) are higher than the strongest absorptions for CD_2=HfH_2 and CH_2=HfD_2 (2 and 7 in Chart 1) as given (3: Hf−H up 11.2 cm^{-1}, Hf−D up 10.9 cm^{-1}. 4: Hf−H up 16.2 cm^{-1}, Hf−D up 8.4 cm^{-1}. 5: Hf−H up 11.1 cm^{-1}, Hf−D up 10.9 cm^{-1}. 6: Hf−H up 16.2 cm^{-1}, Hf−D up 7.5 cm^{-1}).

Additional assignments can be made to counterpart bands of the C=Hf stretch and C−H_2(D_2) wag. The most

(24) (a) Reed, A. J.; Curtiss, L. A.; Weinhold, F. *Chem. Rev.* **1988**, *88*, 899. (b) Frenking, G.; Frohlich, N. *Chem. Rev.* **2000**, *100*, 717.

(25) The *G* matrix elements for symmetric and antisymmetric modes of a MH_2 group are different: $G_{sym} = \mu H + \mu M + \mu M \cos \alpha$ and $G_{antisym} = \mu H + \mu M - \mu M \cos \alpha$, where μ is the reduced (i.e., inverse) mass. Thus for $90° < \alpha < 180°$, the sym mode has less metal and hence more H participation.

Table 3. Observed and Calculated Fundamental Frequencies of CH_2=HfH_2[a]

	CH_2=HfH_2 (1)[b]			CD_2=HfD_2 (8)			$^{13}CH_2$=HfH_2			CD_2=HfH_2 (2)			CH_2=HfD_2 (7)		
description	obs.	calc.	int.	obs.	calc.	int.	obs.	calc.	int.	obs.	calc.	int.	obs.	calc.	int.
ν_1 CH_2 str.		3171.2	1		2344.5	2		3160.6	1		2344.5	2		3171.2	1
ν_2 CH_2 str.		2900.3	7		2111.7	2		2893.5	8		2111.7	3		2900.3	7
ν_3 HfH_2 str. (s)	1614.2	1681.2	237	1153.3	1191.6	119	1614.1	1681.2	237		1681.1	237		1191.6	119
ν_4 HfH_2 str. (a)	1563.6	1653.4	470	1120.9	1174.7	238	1563.5	1653.4	470	1563.4	1653.4	470	1120.9	1174.7	241
ν_5 CH_2 scis.		1312.6	18		1014.5	23		1304.6	17		1014.7	21		1312.3	16
ν_6 C=Hf str.	766.3	751.7	112	684.4	663.1	57	748.0	733.9	117	718.4	695.1	131	754.4	739.0	68
ν_7 CH_2 wag	665.8	668.3	178	534.5	523.8	113	660.6	662.6	175	547.9	541.7	90	666.9	665.3	151
ν_8 HfH_2 bend	632.6	639.5	41		460.8	41	629.6	636.3	31		620.0	11		463.4	37
ν_9 HfH_2 rock		538.7	2		403.1	1		536.0	2		518.7	70		414.9	2
ν_{10} CH_2 twist		404.6	21		287.0	11		404.5	21		323.6	90		379.9	6
ν_{11} HfH_2 wag		315.1	171		225.6	85		314.9	171		300.0	92		230.4	91
ν_{12} CH_2 rock		190.9	11		139.9	7		190.2	10		144.5	7		183.8	10

[a] B3LYP/6-311++G(2d,p)/SDD level. Frequencies and infrared intensities are in cm^{-1} and km/mol. Observed are in argon matrix. Intensities are calculated values. [b] This number gives the isotopic molecule in Chart 1.

Chart 1

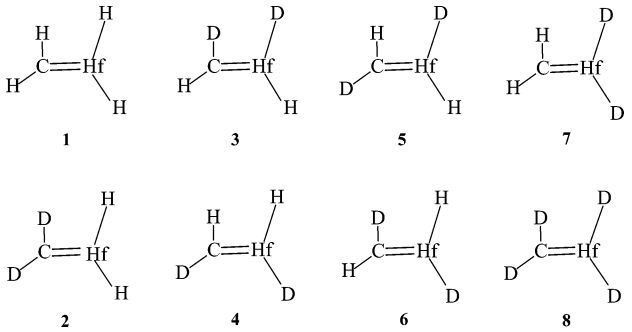

clear-cut of these are bands at 754.4 and 718.4 cm^{-1} that fit calculations for 7 and 2, respectively, and their 7′ and 2′ counterparts at 765.2 and 729.6 cm^{-1}. The CH_2 wag for 7 is identified at 666.9 cm^{-1}. Two other first deposition wagging modes are observed at 555.9 and 547.9 cm^{-1}, but assignment to a particular isotopomer is difficult.

Now, examine the CH_2D_2 product spectra in Figure 4. The major new broader mixed isotopic absorptions at 1579.6 and 1130.7 cm^{-1} are, respectively, 16.2 and 9.8 cm^{-1} higher than the CD_2=HfH_2 and CH_2=HfD_2 absorptions, and the 1129.0 cm^{-1} shoulder absorption is 8.1 cm^{-1} higher. These observations match the predictions for isotopic modifications 4 and 6, and any weaker 3 and 5 counterparts of the first product to be trapped are masked by the wings of the above bands. However, annealing to 20 and 26 K favors the second subgroup, and new mixed isotopic absorptions at 1615.4 and *1606.1* cm^{-1} and at *1157.4* and 1151.1 cm^{-1} (stronger pair italic) are, respectively, 18.9 and *9.6* cm^{-1} higher than the CD_2=HfH_2 absorptions or *12.9* and 6.6 cm^{-1} higher than the CH_2=HfD_2 absorptions. The stronger pair are within 2 cm^{-1} of the harmonic predictions for 3 and 5, and the weaker pair are within 1−3 cm^{-1} of our calculated shifts for 4 and 6. Hence, the clear observation of two extra sets of CHD=HfHD mixed isotopic bands (marked **3′**, **5′** and **4′**, **6′** in Figure 4e) demonstrates the distortion in CH_2=HfH_2 that can be explained by agostic bonding. The shorter Hf−H(D) bond on the same side as the longer (agostic) C−H(D) bond has the higher frequency.

We believe the **1** and **1′** band groups are due to CH_2=HfH_2 in two different argon matrix packing configurations. The Hf reaction with CH_4 is promoted by visible and UV excitation[27] of atomic Hf, and the resulting CH_2=HfH_2 is trapped by argon as characterized by the **1** and **1′** band groups. Visible irradiation reduced the **1′** group in favor of the **1** group, but UV irradiation increased the **1′** set more than the **1** set. Annealing allows a change in this argon cage and favors the **1′** absorptions. We calculate the first Ar to CH_2=HfH_2 binding energy to be 2.6 kcal/mol (MP2), so there is a thermodynamic driving force for matrix cage rearrangement. However, a final UV irradiation restores the original configuration and group **1** absorptions. Two other observations support this hypothesis: The **1** and **1′** band separation is smaller for CH_2=HfH_2 in solid neon and for CH_2=ZrH_2 in solid argon, where the argon packing configuration is also discussed,[10] and the calculated argon complex frequency shifts for Hf−H stretching modes are in reasonable accord with the **1′** and **1** frequency separations.

There is additional information about the agostic structures in Chart 1 from the CH_2D_2 spectra of Figure 4. The initial argon matrix configuration surrounding CH_2=HfH_2 (1563.4 cm^{-1} band denoted **1**) gives rise to mostly isotopomers 2, 7, and 4 or 6 based on shifted bands in both Hf−H and Hf−D stretching regions. However, on annealing to 20 K the 1597.1 cm^{-1} band (labeled **2′**) emerges with a different argon matrix packing environment and both 4, 6 and 3, 5 isotopomers are observed, but now the latter 3, 5 bands are more intense (Figure 4d). On annealing to 26 and 32 K, this preference for the 3, 5 over the 4, 6 isotopomers becomes even more pronounced (Figure 4e,f). Our spectra show that the agostic C−H(D) and Hf−H(D) positions switch on annealing of CHD=HfHD isotopomers. In other words, annealing allows a 4, 6 → 3, 5 isotopic isomerization, which amounts to an exchange in the elongated agostic C−H(D) bond and shorter Hf−H(D) bond positions. This is observed in the infrared spectrum through an increase in the **3′**, **5′** band relative to the **4′**, **6′** band absorbance on annealing (Figure 4d,e,f).

Intrinsic reaction coordinate (IRC) calculations[26] were done to estimate the barrier to exchange of agostic positions. This barrier is computed as 0.2 kcal/mol at the B3LYP level or 2.3 kcal/mol at the MP2 level (large basis set), and the truth is somewhere in between. On annealing, argon matrix packing configurations change because of an attractive CH_2=HfH_2- - -Ar binding en-

(26) Gonzalez, C.; Schlegel, H. B. *J. Phys. Chem.* **1990**, *94*, 5523.
(27) Chertihin, G. V.; Andrews, L. *J. Phys. Chem.* **1995**, *99*, 15004.

Table 4. Observed and Calculated Fundamental Frequencies of $(CH_3)_2HfH_2$[a]

	$(CH_3)_2HfH_2$			$(CD_3)_2HfD_2$			$(^{13}CH_3)_2HfH_2$		
description	obs.	calc.	int.	obs.	calc.	int.	obs.	calc.	int.
A HfH_2 str.	1657.3	1700.8	299	1184.7	1205.4	153	1657.2	1700.8	299
B HfH_2 str.	1626.6	1669.1	513	1165.4	1185.9	262	1626.5	1669.1	513
B CH_3 bend	1377.8	1422.6	17		1031.9	11	1374.3	1419.5	17
B CH_3 deform	1142.2	1179.3	33		928.0	55	1131.6	1169.3	29
B HfH_2 wag	570.0	574.8	221		462.1	126	566.8	571.1	215

[a] B3LYP/6-311++G(2d,p)/SDD level. Frequencies and infrared intensities are in cm^{-1} and km/mol. Observed are in argon matrix. Intensities are calculated values.

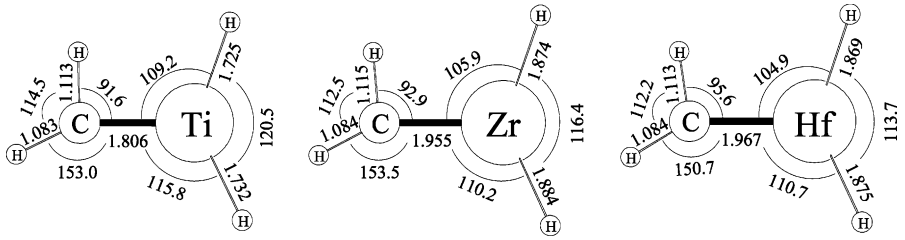

Figure 7. Structures computed for methylidene group 4 dihydride complexes using B3LYP/6-311++G(3df, 3dp)/SDD metal.

Table 5. Natural Bond Orbital Analysis for Group 4 Methylidene Dihydride Complexes[a]

parameters[b]	$CH_2{=}TiH_2$	$CH_2{=}ZrH_2$	$CH_2{=}HfH_2$
q (C)	−0.86	−1.04	−1.15
q (H_3)	0.20	0.20	0.20
q (H_4)	0.18	0.19	0.19
q (M)	1.28	1.54	1.66
q (H_5)	−0.39	−0.45	−0.46
q (H_6)	−0.41	−0.43	−0.45
M	$4s^{0.42}\ 3d^{2.31}$	$5s^{0.42}\ 4d^{2.08}$	$6s^{0.55}\ 5d^{1.82}$
C	$2s^{1.29}\ 2p^{3.55}$	$2s^{1.30}\ 2p^{3.72}$	$2s^{1.31}\ 2p^{3.82}$
H_3	$1s^{0.80}$	$1s^{0.80}$	$1s^{0.79}$
H_4	$1s^{0.82}$	$1s^{0.81}$	$1s^{0.81}$
H_5	$1s^{1.40}$	$1s^{1.44}$	$1s^{1.45}$
H_6	$1s^{1.38}$	$1s^{1.43}$	$1s^{1.44}$

[a] Calculations: B3LYP/6-311++G(3df,3pd)/SDD. [b] Natural charges and electron configurations. H atom numbers in Figure 6.

ergy (2.6 kcal/mol, MP2). Hence, the coordination of additional argon atoms provides more than enough energy to activate exchange of agostic positions and to repartition the CHD=HfHD isotopomers, which demonstrates facile interchange of the agostic bonding positions. Finally, the above transition state is just the symmetrical (C_s) nonagostic $CH_2{=}HfH_2$ molecule, which is 2.3 kcal/mol higher in energy than the agostic ground state at the MP2 level, which provides an estimate of the agostic distortion stabilization for $CH_2{=}HfH_2$.

$(CH_3)_2HfH_2$. The two **di** bands are enhanced over the **1** bands in experiments using higher CH_4 concentration, and they increase markedly on sample annealing (Figure 1e,f). With the CH_2D_2 precursor the two **di** bands acquire a stronger intermediate component (Figure 4). This is the behavior expected for symmetric and antisymmetric Hf−H_2 and Hf−D_2 stretching modes on HfHD substitution where single intermediate Hf−H and Hf−D modes are observed. The **di** bands exhibit 1657.3/1184.5 = 1.399 and 1626.6/1163.4 = 1.398 H/D ratios and virtually no ^{13}C shifts. Similar behavior was found for the analogous $(CH_3)_2ZrH_2$ moelcule.[9,10]

Three other diagnostic vibrational modes involving methyl hydrogen and metal hydride bending were observed for $(CH_3)_2HfH_2$, as summarized in Table 4. The comparison of calculated and observed isotopic frequencies and the slightly lower frequency $(CH_3)_2ZrH_2$ counterparts[9,10] substantiate this identification of $(CH_3)_2HfH_2$. The scale factors (observed/calculated frequencies) for $CH_2{=}HfH_2$ (0.960, 0.946) and $(CH_3)_2HfH_2$ (0.974, 0.975) Hf−H stretching modes are in accord with scale factors for other transition metal compounds.[10] Our calculations overestimate the intensity of HfH_2 bend and wag modes relative to CH_3 bend and deformation modes. The antisymmetric Hf−H_2 stretching mode for $(CH_3)_2HfH_2$ (1626.6 cm^{-1}) may be compared with those for HfH_4 (1678.4 cm^{-1}) and HfH_2 (1622.4 cm^{-1}) in solid argon,[27] and with $(Cp^*)_2HfH_2$ (1590 cm^{-1}).[19]

We calculated $CH_3{-}HfH_3$ frequencies to check for this possible product with a very strong Hf−H_3 stretching mode, and we find no other strong absorption in the predicted region. Finally, we do not observe HfH_2 or HfH_4 in these experiments, so insufficient H_2 is produced to give reaction products.

Agostic Bonding. Figure 7 illustrates structures for the group 4 methylidene dihydrides and shows that the distortion involved in agostic bonding decreases from the Ti to the Hf species. This may be due in part to the longer C=Hf double bond. A similar relationship has been found in the $CH_2{=}MHF$ substituted methylidenes.[14−16] The natural bond orbital analysis (Table 5) gives negative carbon and positive metal natural charges which increase, giving more C=M bond polarity going down the family. This increase in polarity for hafnium methylidene has been noted previously along with the prediction of increased catalytic activity for alkene methathesis.[8] Following this trend, the natural electron configurations show an increase in carbon 2p with a corresponding decrease in metal nd populations. The electron configurations on the hydrogens are relatively constant. We think of the agostic interaction involving a C−H bond and an electron-deficient transition metal center. The CH_2 subunit deforms and the C=Hf double bond is stabilized in the agostic bonding process.[28,29]

(28) Scherer, W.; McGrady, G. S. *Angew. Chem., Int. Ed.* **2004**, *43*, 1782.

(29) Clot, E.; Eisenstein, O. Agostic Interactions from a Computational Perspective. *Structure and Bonding, Computational Inorganic Chemistry*; Kaltzoyannis, N., McGrady, J. E., Eds.; Springer-Verlag: Heidelberg, 2004; pp 1−36.

Reaction Mechanisms. We propose that excited Hf activates methane to give the energized hydride, which undergoes α-H transfer[30] to the methylidene before relaxation in the argon matrix. Our B3LYP calculations (Table S1) find the CH_3HfH and $CH_2{=}HfH_2$ molecules to have almost the same binding energy, and reaction 1 is exothermic with $\Delta E = -22$ kcal/mol (B3LYP), but $CH_2{=}HfH_2$ is 10.6 kcal/mol more stable at the MP2 level. Apparently α-H transfer is very fast in the energized $[CH_3{-}Hf{-}H]^*$ intermediate, as only the $CH_2{=}HfH_2$ product is trapped.

$$Hf^* + CH_4 \rightarrow [CH_3{-}Hf{-}H]^* \rightarrow [CH_2{-}HfH_2]^* \rightarrow CH_2{=}HfH_2 \quad (1)$$

The methylidene activates another methane molecule to form the stable dimethyl hafnium dihydride in exothermic reaction 2 with computed $\Delta E = -51$ kcal/mol. This happens on annealing in solid argon (20−26 K), which implies essentially zero activation barrier.

$$CH_2{=}HfH_2 + CH_4 \rightarrow (CH_3)_2HfH_2 \quad (2)$$

The analogous reaction 3, which we have not observed here, has a computed $\Delta E = -52$ kcal/mol.

$$CH_2{=}HfH_2 + H_2 \rightarrow CH_3{-}HfH_3 \quad (3)$$

Family Relationships. The most interesting group 4 trend is the decrease in agostic bonding interaction in the $CH_2{=}MH_2$ methylidene complexes on going down the family, as discussed above. Note that this follows an increase in C=M bond length. On the other hand, the activation of a second methane molecule is more exothermic (ΔE for reaction 2 is −37, −44, and −51 kcal/mol for Ti, Zr, and Hf, respectively),[10,11] which points to an increase in relative stability for the dimethyl metal dihydride going down the family. Our computed simple C=M bond lengths (Figure 7) are slightly shorter than those measured for ligated Ti, Zr, and Hf methylidene complexes, 1.884, 2.024, and 1.994 Å, respectively.[13,31,32]

Although the CH_3TiH insertion product was clearly observed for Ti, where this isomer is 22 kcal/mol more stable than $CH_2{=}TiH_2$,[11] a tenuous observation of CH_3ZrH was made,[10] where CH_3ZrH is computed to be only 3 kcal/mol more stable than $CH_2{=}ZrH_2$, and we have no evidence for CH_3HfH, which is isoergic with $CH_2{=}HfH_2$ (B3LYP level). We also observe that the total yield of products increases from Ti to Zr to Hf, which points to a greater reactivity for Hf.

Note the relativistic contraction of Hf−H bond lengths relative to Zr−H bond lengths. This was predicted over 25 years ago by Pyykko et al.,[33−36] and higher vibrational frequencies have been observed for HfH_2, HfH_4 than for ZrH_2, ZrH_4.[27] However, note that the computed C=Hf bond is slightly longer than the corresponding C=Zr bond: This may arise from smaller relativistic contraction for p electrons, and thus multiple bonds, than s electrons and single bonds.

A final family relationship to consider is the separation between **1** and **1′** absorptions for argon matrix packing configurations. For $CH_2{=}TiH_2$ this separation is 6.9 cm^{-1}, which is in line with argon matrix site splittings. However, this separation increases to 20.5 cm^{-1} for $CH_2{=}ZrH_2$ and to 33.5 cm^{-1} for $CH_2{=}HfH_2$, which requires more explanation. We suggest that the larger more diffuse Hf 5d orbitals allow attractive interaction with more Ar atoms than the correspondingly smaller Zr 4d and Ti 3d orbitals, and this accounts for the larger matrix coordination shift.

Conclusions

Laser-ablated Hf atoms react with CH_4 to produce the simple hafnium carbene hydride complex $CH_2{=}HfH_2$, which is identified by Hf−H stretching absorptions at 1614.2 and 1563.6 cm^{-1}, a mostly C=Hf stretching mode at 766.3 cm^{-1}, and a CH_2 wagging mode at 665.8 cm^{-1}. These assignments are supported by isotopic substitution (CH_4, $^{13}CH_4$, CD_4, CH_2D_2) and B3LYP isotopic frequency calculations. The structure computed for $CH_2{=}HfH_2$ shows considerable CH_2 distortion and evidence of agostic bonding and is 2.3 kcal/mol (MP2) more stable than the symmetrical structure, which produces an estimate of the agostic stabilization energy. In addition the CHD=HfHD isotopic molecules provide experimental evidence for agostic bonding distortion and interchange of the agostic bonding positions on annealing the argon matrix to 20−26 K. This suggests that the binding of more Ar to Hf activates the interchange of agostic bonding positions. The reaction of a second CH_4 molecule forms $(CH_3)_2HfH_2$, which appears to have essentially no activation energy requirement, and is, we believe, the first preparation of a methyl hafnium hydride.

Acknowledgment. We gratefully acknowledge financial support from N.S.F. Grants CHE 00-78836 and CHE 03-52487, sabbatical leave support (H.-G.C.) from the Korea Research Foundation (KRF-2003-013-C00044), and helpful correspondence with P. Pyykko, G. S. McGrady, and O. Eisenstein.

OM050069L

(30) Crabtree, R. H. *The Organometallic Chemistry of the Transition Metals*; Wiley and Sons: New York, 2001; p 190.
(31) Fryzuk, M. D.; Mao, S. S. H.; Zaworotko, M. J.; McGillivray, L. R. *J. Am. Chem. Soc.* **1993**, *115*, 5336.
(32) Baumann, R.; Stumpf, R.; Davis, W. M.; Liang, L.-C.; Schrock, R. R. *J. Am. Chem. Soc.* **1999**, *121*, 7822.
(33) Pyykko, P.; Desclaux, J. P. *Chem. Phys. Lett*. **1977**, *50*, 503.
(34) Pyykko, P.; Snijders, J. G.; Baerends, E. *J. Chem. Phys. Lett*. **1981**, *83*, 432.
(35) Ziegler, T.; Snijders, J. G.; Baerends, E. J. *J. Chem. Phys*. **1981**, *74*, 1271.
(36) Pyykko, P. *Chem. Rev*. **1988**, *88*, 563.